When micro-swimmers get a spring in their stroke

When micro-swimmers get a spring in their stroke

Jayant Pande[1], Laura Merchant[1,2], Jens Harting[3,4] and Ana-Sunčana Smith[1,5,*]
[1]*Institute for Theoretical Physics and Cluster of Excellence: EAM, Friedrich-Alexander University Erlangen-Nuremberg, Erlangen, Germany;* [2]*School of Physics and Astronomy, University of St. Andrews, St. Andrews, Scotland;* [3]*Department of Applied Physics, Eindhoven University of Technology, Eindhoven, the Netherlands;* [4]*Faculty of Science and Technology, Mesa+ Institute, University of Twente, Enschede, the Netherlands;* [5]*Division of Physical Chemistry, Ruđer Bošković Institute, Zagreb, Croatia.*[*]

(Dated: November 24, 2014)

The fundamental mechanisms underlying swimming at the micro-scale have important consequences on biological systems or the fabrication of micro-fluidic devices. In this analytical work we demonstrate that a mechanical bead-spring micro-swimmer can undergo two regimes of swimming, where the swimming velocity decreases or counter-intuitively increases with the viscosity. We show that it is the elasticity of a mechanical micro-swimmer which dictates this crucial phenomenon. Furthermore, it is generally ignored in the literature that naturally occurring swimmers are often flexible. To model this phenomenon, we allow the beads of our micro-swimmer to be weakly deformable and show that such flexibility also leads to a positive or negative impact on the propulsion of the swimmers.

PACS numbers: 47.63.Gd, 47.63.mh, 87.85.Tu

The study of micro-swimmer motion has gained a lot of impetus recently, driven in equal measure by advances in experimental technology [1–12], numerical methods [13–17], and theoretical modelling [18–24]. The increased analysis has served to highlight the dazzling variety of ways in which nature accomplishes the difficult task of achieving non-reversibility of motion in spite of sparsity of material [25]. These greatly varied natural swimming mechanisms are nevertheless mostly mechanical, in that the motion is driven by different parts of the swimmer body moving in coordinated yet asymmetric ways, leading to a corresponding asymmetry in the surrounding flow field. For artificial swimmers, on the other hand, chemically-driven mechanisms are as popular as mechanical ones [26–32].

Physically, it is clear that the body deformations in mechanical swimmers, which consist of rotation and translation of different surface elements leading to the contraction and expansion of different body parts, can be modelled as elastic degrees of freedom. For instance, the numerical modelling of cilia and flagella, two of the most common swimming appendages in natural micro-swimmers, has been successfully based on replacing them with linear arrangements of tiny links with elastic forces including bending and stretching at the joints [14, 33]. Other motions, such as peristalsis in Euglena, are more properly modelled as tubes with elastic deformations running down them [34]. Therefore, elasticity may be said to be the fundamental property enabling motility in many natural and artificial swimmers.

Motivated by this, we here discuss the general effects of elasticity in micro-swimming, a task that has not been attempted so far. Our investigations lead to the remarkable result that there are two viscosity-dependent regimes in micro-swimming, where the velocity is promoted or suppressed by an increase in the fluid viscosity, depending on the swimmer elasticity. This may help to explain why some swimmers can speed up in more viscous fluids [35–38]. In addition, we investigate whether more efficient swimming motion results from rigid construction material–apart from the elastic driving component–or deformable material. We show that the answer again hinges on the precise value of the swimmer's elasticity.

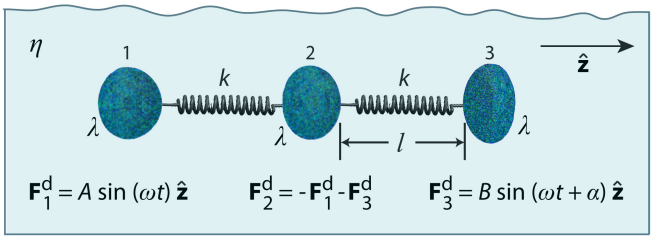

FIG. 1. (Color online) A three-bead swimmer with rigid or deformable beads.

We base our model swimmer on the popular three-sphere design [39, 40], which is widely accepted in the community as being ideal for elucidating the general principles of micro-swimming. In our model, however, we use three beads of variable flexibility that are connected by two harmonic springs of arbitrary stiffness. We also stipulate the forces driving the swimming motion, allowing the swimming stroke to respond dynamically to the forces instead of being pre-assumed as in the originating paper [39]. Apart from being arguably more *ab initio*, this approach has the important advantage of allowing us to evaluate separately the effect upon the swimming of the different forces, namely the spring forces, the driving forces and the hydrodynamic forces, which is crucial to our study.

We assume the driving forces to be sinusoidal, given by

$$\begin{aligned} &\mathbf{F}_1^{\mathrm{d}}(t) = A\sin(\omega t)\,\hat{\mathbf{z}}; \quad \mathbf{F}_2^{\mathrm{d}}(t) = -\mathbf{F}_1^{\mathrm{d}}(t) - \mathbf{F}_3^{\mathrm{d}}(t); \\ &\mathbf{F}_3^{\mathrm{d}}(t) = B\sin(\omega t + \alpha)\,\hat{\mathbf{z}}, \text{ with } \alpha \in [-\pi, \pi]. \end{aligned} \tag{1}$$

Here A and B are non-negative amplitudes of the time-dependent driving forces $\mathbf{F}_1^{\mathrm{d}}(t)$ and $\mathbf{F}_3^{\mathrm{d}}(t)$ applied along the

$\hat{\mathbf{z}}$-direction to the outer beads at the frequency ω and with the phase difference α. The force $\mathbf{F}_2^{\rm d}(t)$ on the middle bead is set by the condition for autonomous propulsion, which requires the net driving force on the device to vanish at all times. Each spring, aligned along $\hat{\mathbf{z}}$, has a stiffness constant k and a rest length l (Fig. 1), with l much larger than the bead dimensions.

As micro-swimming typically takes place in the Stokes regime, the fluid is assumed to be governed by the Stokes equation $\eta\nabla^2\mathbf{u}(\mathbf{r},t)-\nabla p(\mathbf{r},t)+\mathbf{f}(\mathbf{r},t)=0$ and the incompressibility condition $\nabla\cdot\mathbf{u}=0$. Here η is the dynamic viscosity of the fluid moving with a velocity $\mathbf{u}(\mathbf{r},t)$ under a pressure $p(\mathbf{r},t)$ at the point $\mathbf{r}$ at time t. The force density $\mathbf{f}(\mathbf{r},t)$ acting on the fluid is given by

$$\mathbf{f}(\mathbf{r},t)=\sum_{i=1}^{3}\left[\mathbf{F}_i^{\rm d}(t)+\mathbf{F}_i^{\rm s}(t)\right]\delta\left(\mathbf{r}-\mathbf{R}_i(t)\right), \qquad (2)$$

where the index $i=1,2,3$ denotes the i-th bead placed at the position $\mathbf{R}_i(t)$ subject to a driving force $\mathbf{F}_i^{\rm d}(t)$ and a spring force $\mathbf{F}_i^{\rm s}(t)$ (which, for the middle bead, results from two springs). Assuming no slip at the fluid-bead interfaces, the instantaneous velocity $\mathbf{v}_i(t)$ of each bead [41] is given by

$$\mathbf{v}_i=\frac{{\rm d}\mathbf{R}_i}{{\rm d}t}=\left(\mathbf{F}_i^{\rm d}+\mathbf{F}_i^{\rm s}\right)\gamma^{-1}+\sum_{j\neq i}^{3}\mathbf{T}\left(\mathbf{R}_i-\mathbf{R}_j\right)\cdot\left(\mathbf{F}_i^{\rm d}+\mathbf{F}_i^{\rm s}\right), \quad (3)$$

with γ being the Stokes drag coefficient [42, 43] and $\mathbf{T}(\mathbf{r})$ the Oseen tensor [44, 45]. The latter is here diagonal, due to the collinear nature of the driving forces and the employed far-field approximation (bead dimensions much smaller than l).

We define a 'reduced drag coefficient' of the beads, $\lambda=\gamma/(6\pi\eta)$, and an 'effective elastic parameter', $\psi=k/(\pi\omega\lambda)$. The far field approximation translates to $\lambda\ll l$. As discussed in Ref. [46], the steady state bead positions can be written as

$$\mathbf{R}_i(t)=\mathbf{S}_{i0}+\boldsymbol{\xi}_i(t)+\mathbf{v}t \qquad (4)$$

due to the sinusoidal nature of the forces. Here $\boldsymbol{\xi}_i(t)$ denotes small sinusoidal oscillations around the equilibrium configuration $\mathbf{S}_{i0}$ of the device. $\mathbf{S}_{i0}$ moves with a uniform swimming velocity $\mathbf{v}$, obtained by integrating $\tau^{-1}[\sum_{i=1}^{3}(\mathbf{v}_i/3)]$ over the time period τ of one cycle.

Rigid beads.—Eqs. (3) and (4) lead to differential equations in the $\boldsymbol{\xi}_i$'s ([46]), which we solve under the assumption of small oscillations, *i.e.* $|\boldsymbol{\xi}_i(t)|\ll l$ for all i and all times t. Since the forces and the displacements are all sinusoidal, the first-order terms in the perturbation variable $\boldsymbol{\xi}_i(t)$ turn out to be zero. The velocity expression for swimmers with rigid beads, accurate to the second order in $\boldsymbol{\xi}_i$, is

$$\mathbf{v}_{\rm r}=\frac{7\left[AB\left(\psi^2+12\eta^2\right)\sin\alpha+2\left(A^2-B^2\right)\psi\eta\right]}{24\lambda l^3\pi^2\omega\left(\psi^2+4\eta^2\right)\left(\psi^2+36\eta^2\right)}\hat{\mathbf{z}}. \qquad (5)$$

The model allows one to include beads of any shape whose friction coefficient λ is known. In the appropriate limits ($\lambda\ll l$ and $|\boldsymbol{\xi}_i(t)|\ll l$), Eq. (5) can actually be cast in a stroke-centric form, $\mathbf{v}=Gd_1d_2\omega\sin\beta\hat{\mathbf{z}}$, where G is a geometric factor, d_1 and d_2 are the amplitudes of the oscillations of the swimmer's arms, and β gives the phase difference between the two [40]. In our approach, d_1, d_2 and β emerge as explicit functions of the different driving and swimmer parameters.

While the natural expectation is for the velocity $\mathbf{v}_{\rm r}$ to decrease with the viscosity η ('conventional' regime), Eq. (5) leads to the remarkable result that $\mathbf{v}_{\rm r}$ is a non-monotonic function of η (Fig. 2 (a), (b)). As such, together with the conventional regime, there is an 'aberrant' regime where $\mathbf{v}_{\rm r}$ increases with η. Interestingly, the change between these regimes, marked by an appearance of extrema in the velocity-viscosity curves, is concurrent with a change in the pusher or puller nature of the swimmer, determined by the relation

$$\left(\frac{B}{A}-\frac{A}{B}\right)^{-1}\sin\alpha\gtrless\frac{2\psi\eta}{\psi^2+12\eta^2}. \qquad (6)$$

When the left hand side of relation (6) is larger (smaller), then the swimmer moves in the direction of the bead with the higher (lower) force amplitude, and the swimmer is consequently a puller (pusher). These intrinsic phenomena are a consequence of the interplay of the drag forces on the swimmer and its elastic degrees of freedom.

For a three-bead swimmer of a fixed elastic parameter ψ and varying viscosity η, it can be shown that if the driving parameters satisfy the relation $(A-B)/\sin\alpha>0$, then the swimmer is a pusher and the velocity $\mathbf{v}_{\rm r}$ as a function of η has exactly one extremum (Fig. 2(a)). This maximum divides the conventional regime (shaded in yellow in Fig. 2(a)) and the aberrant regime (dark green), the latter being confined to a region asymptotically bounded by the lines $\eta=\psi/(2\sqrt{5+2\sqrt{13}})$ and $\mathbf{v}_{\rm r}=\mathbf{v}_{\rm r}|_{A=B}$.

If $(A-B)/\sin\alpha<0$, then the velocity has zero or several (2 or 4) local extrema (Fig. 2(b)). In the former case the swimmer is in the conventional regime for all values of the viscosity and is always a puller (yellow dashed curve in Fig. 2(b)). However, if $B>A(1+6\sin^2\alpha+2\sin\alpha\sqrt{3+9\sin^2\alpha})^{1/2}$, then a swimmer with a fixed elastic parameter becomes aberrant for an intermediate range of viscosities (solid yellow-green curve in Fig. 2(b)) and can be a pusher.

We summarize these results showing the conventional and the aberrant regimes in phase diagrams (Fig. 2(c), yellow and green regions, respectively) which are constructed for a fixed value of the viscosity η and increasing values of the effective elastic parameter ψ. We find that when swimmers change between these regimes, their pusher or puller nature (shown in pink and blue, respectively) also usually changes. At small ψ values, pullers are aberrant, except in a small region at the boundary of pushers and pullers where they are conventional. For pushers, if $(A-B)/\sin\alpha<0$ then the swimming is conventional, otherwise it is aberrant. This holds true until the critical value $\psi_c=2\sqrt{5+2\sqrt{13}}\eta$. When ψ increases beyond ψ_c, then all pullers become aberrant, as do all pushers for which $(A-B)/\sin\alpha<0$. If this latter relation does not hold, then pushers may be conventional or aberrant. Ultimately, at large values of the elastic parameter ψ, the conventional and the aberrant regimes each occupy half of the phase space.

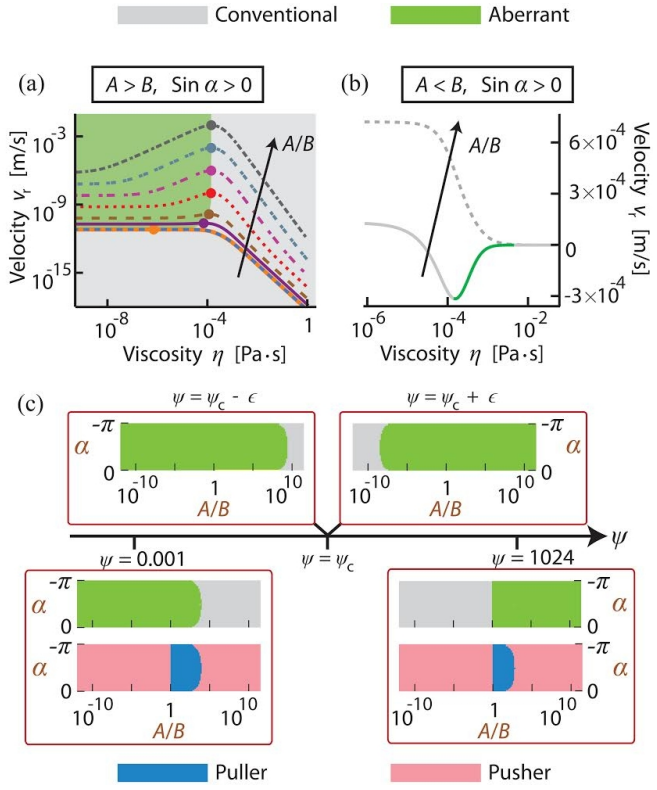

FIG. 2. (Color online) For swimmers with rigid beads. (a) Velocity vs. viscosity curves for different values of A/B (ranging from 1 to 10^5), with $A > B$ and $\sin\alpha = 1$. The large dots mark the maxima. (b) Velocity vs. viscosity curves with $A < B$ and $\sin\alpha = 1$. The value of A/B for the two curves is 0.05 and 0.91. (c) Phase diagrams for different values of the forcing parameters α, A and B, as well as the corresponding puller or pusher nature of the swimmer. The value of η is kept fixed at 1.0, and ψ is varied between the different plots. The critical elastic parameter value ψ_c is 6.99. Note that the phase diagrams do not depend on the particular value of η used, as the η values where the velocity has extrema are proportional to ψ. Therefore, for any other viscosity value, one only needs to change the ψ values by the same factor to obtain the same phase diagrams.

Swimmers with flexible beads.–The harmonic springs considered so far may represent any elastic degrees of freedom that affect the motion of neighboring body parts. However, it is possible for a particular structural element in a swimmer to possess flexibility that in the absence of the surrounding fluid do not affect the other degrees of freedom. Such elements clearly contribute to self-propulsion as evidenced by a two-bead assembly, which is able to swim only if the bead shapes are allowed to change [21]. However, it remains to be clarified under which conditions flexibility promotes or hinders swimming. To address this question we allow each bead to undergo small but arbitrary fluctuations around an average shape. The instantaneous effective drag coefficient $\lambda_i(t)$ can be expressed in a Fourier series in ωt,

$$\lambda_i(t) = a_i + \sum_{n=1}^{\infty} b_i^n \sin\left(n\omega t + \phi_i^n\right), \quad i = 1,2,3. \tag{7}$$

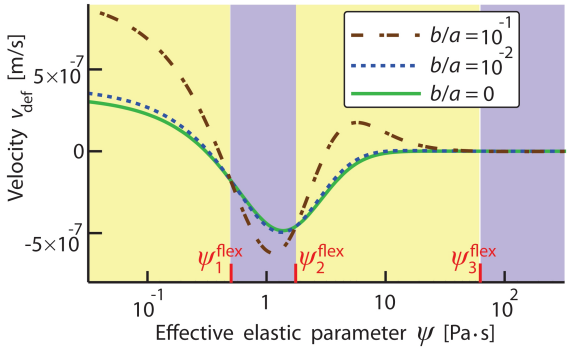

FIG. 3. (Color online) Velocity vs. effective elastic parameter for swimmers with flexible beads. The light yellow and violet colors mark regions where the velocity increases and decreases with the bead flexibility b, respectively. The solid green curve is for a swimmer with rigid beads.

Here a_i is the effective drag coefficient of the mean shape, and b_i^n and ϕ_i^n are the amplitude and the phase shift of the contribution from the n-th frequency mode. The oscillations of the effective drag coefficient are supposed to be weak and of no bigger order than the oscillations $\xi_i(t)$ of the arm lengths ($b_i^n \ll a_j \ll l_k$ and $b_i^n \lesssim |\boldsymbol{\xi}_j| \ll l_k$, for all i,j,k,n). This assumption ignores the agitation of the fluid due purely to the shape deformations, and the change in a bead's radius only affects its own motion, not that of the other beads.

The bead flexibility makes the full drag coefficient γ in Eq. (3) time-dependent. We can still solve Eqs. (3) and (4), to the first order in b_i^j/a_k and the second order in $\boldsymbol{\xi}_i$, by ignoring terms of the form $b_i^j \boldsymbol{\xi}_k^2$, since $b_i^n \lesssim |\boldsymbol{\xi}_j|$ by assumption. Due to the coupling of each mode with sinusoidal forces and bead displacements in the integral equations of motion, and the orthogonality of sine functions, we find that only the frequency mode in the Fourier series expansion that matches the driving force frequency ($n = 1$) contributes to the swimmer velocity. Consequently, the velocity of a swimmer with deformable bodies adopts the form

$$\mathbf{v}_{\rm def} = \mathbf{v}_{\rm r} + \sum_{i=1}^{3} \mathbf{m}_i b_i^1. \tag{8}$$

Here the coefficients $\mathbf{m}_i$ do not contain the shape deformation amplitudes b_j^1 and may be positive or negative. The full velocity expression is in the Supplemental Material (S.M.) in the form of a *Mathematica* file. The difference between the rigid bead and the flexible bead cases is highlighted with symmetric driving ($A = B$ and $\alpha = 0$), where $\mathbf{v}_{\rm r} = \mathbf{0}$ but $\mathbf{v}_{\rm def} \neq \mathbf{0}$. If $\mathbf{m}_i$ is positive (negative), then clearly the velocity increases (decreases) with b_i^1. If the net effect of these terms is positive, then the swimmer is in the 'flexibility-enhanced' regime of self-propulsion, otherwise in the 'flexibility-reduced' regime .

We identify these two regimes for the special case of a swimmer with $b_i^1 = b$ and $a_i = a$, for $i = 1,2,3$. Then one can show that there are up to three critical values of the effective elastic parameter $\psi_i^{\rm flex}$ (see S.M. for *Mathematica* files)

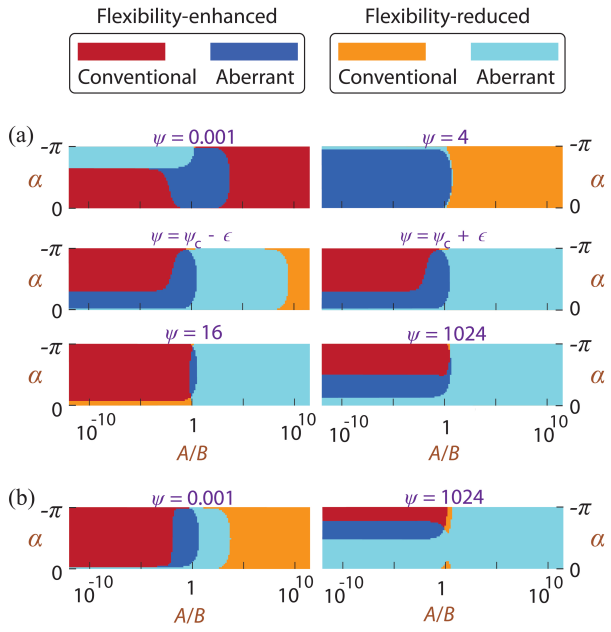

FIG. 4. (Color online) (a) Phase diagrams for swimmers with flexible beads, for different values of the forcing parameters α, A and B. The value of η is kept fixed at 1.0, and ψ is varied between the different plots. ψ_c is 6.99. The bead flexibility b/a is 10^{-3}, and the phase shifts in the shape deformation of the three beads are $\phi_1^1 = \pi/3$, $\phi_2^1 = \pi/7$ and $\phi_3^1 = \pi/1.8$. (b) Two of the plots from part (a) when ϕ_2^1 is increased tenfold to $10\pi/7$.

that separate regions of flexibility-enhanced ($\mathrm{d}v_r/\mathrm{d}b > 0$) and flexibility-reduced ($\mathrm{d}v_r/\mathrm{d}b < 0$) regimes, as shown in Fig. 3. Since one of the ψ_i^{flex}'s is always real and positive, both regimes exist for every choice of the effective elastic parameter ψ. Knowledge of ψ, therefore, is sufficient to determine how the swimmer velocity would change with a change in the bead flexibility, no matter what the value of this flexibility is.

Finally, we can investigate the effect of the bead flexibility together with the swimmer's response to changes in the viscosity. Since both of these effects are sensitive to the effective elastic parameter of the swimmer, we construct a set of phase diagrams (Fig. 4) analogous to those shown in Fig. 2(c). Here the flexibility b/a as well as the viscosity η are kept fixed. The diagrams show that flexibility changes the position of the phase boundaries between the aberrant and the conventional regimes. For $\psi \ll \psi_c$ the region occupied by the aberrant regime (whether flexibility-reduced or enhanced) decreases in area when compared to the rigid bead case. In contrast, for $\psi \gg \psi_c$ the conventional regime decreases in area. Close to $\psi = \psi_c$ either of the two regimes may gain in area on making the beads more flexible. The precise boundaries between the regimes depend greatly on the precise values of the flexibility b/a as well as the shape deformation phase differences ϕ_i^1 (compare parts (a) and (b) in Fig. 4, where ϕ_2^1 is different by a factor of 10).

Conclusion.—By using a simple model that allows analytical treatment, we have studied the effect of elasticity on micro-swimming. Contrary to conventionally expected behavior, we have discovered a swimming regime where the velocity increases as a function of the fluid viscosity, in addition to the more commonly encountered regime where it decreases. This is a consequence of the ways in which the swimmer elasticity, the fluid viscosity and the drag force on the swimmer couple, and may provide a purely physical explanation of why some natural swimmers swim more efficiently in more viscous fluids. Furthermore, we have discovered that flexible degrees of freedom which are not involved in the swimming mechanism can also either enhance or counteract the motion, with their effect again being dependent on the swimmer's dominant elasticity. Our study not only provides new insight into the role of elastic degrees of freedom in micro-swimming, which are nearly ubiquitous, but also gives pointers for the construction of more efficient practical realizations of a micro-swimmer.

Acknowledgment.—A.-S. S. and J. P. thank KONWIHR ParSwarm and ERC-2013-StG 337283 MembranesAct grants for financial support. J. H. acknowledges support by NWO/STW (Vidi grant 10787) and L. M. thanks the DAAD for a RISE scholarship. We are also grateful to K. Pickl, H. Köstler and K. Mecke for helpful discussions.

* smith@physik.uni-erlangen.de

[1] R. Dreyfus, J. Baudry, M. L. Roper, M. Fermigier, H. A. Stone and J. Bibette, *Nature*, 2005, **437**, 862.
[2] K. Ishiyama, M. Sendoh, A. Yamazaki and K. I. Arai, *Sensor Actuat. A-Phys.*, 2001, **91**, 141.
[3] J. J. Benkoski, J. L. Breidenich, O. M. Uy, A. T. Hayes, R. M. Deacon, H. B. Land, J. M. Spicer, P. Y. Keng and J. Pyun, *J. Mater. Chem.*, 2011, **21**, 7314.
[4] Y.-H. Li, S.-T. Sheu, J.-M. Pai and C.-Y. Chen, *J. Appl. Phys.*, 2012, **111**, 07A924.
[5] J. L. Breidenich, M. C. Wei, G. V. Clatterbaugh, J. J. Benkoski, P. Y. Keng and J. Pyun, *Soft Matter*, 2012, **8**, 5334.
[6] L. Baraban, D. Makarov, R. Streubel, I. Mönch, D. Grimm, S. Sanchez and O. G. Schmidt, *ACS Nano*, 2012, **6**, 3383.
[7] L. Baraban, M. Tasinkevych, M. N. Popescu, S. Sanchez, S. Dietrich and O. G. Schmidt, *Soft Matter*, 2012, **8**, 48.
[8] N. C. Keim, M. Garcia and P. E. Arratia, *Phys. Fluids*, 2012, **24**, 081703.
[9] I. Theurkauff, C. Cottin-Bizonne, J. Palacci, C. Ybert and L. Bocquet, *Phys. Rev. Lett.*, 2012, **108**, 268303.
[10] T. Sanchez, D. Welch, D. Nicastro and Z. Dogic, *Science*, 2011, **333**, 456.
[11] Q. Liao, G. Subramanian, M. P. DeLisa, D. L. Koch and M. Wu, *Phys. Fluids*, 2007, **19**, 061701.
[12] M. Leoni, J. Kotar, B. Bassetti, P. Cicuta and M. C. Lagomarsino, *Soft Matter*, 2009, **5**, 472.
[13] C. M. Pooley, G. P. Alexander and J. M. Yeomans, *Phys. Rev. Lett.*, 2007, **99**, 228103.
[14] J. Elgeti and G. Gompper, *Proc. Natl. Acad. Sci. U.S.A.*, 2013, **110**, 4470.
[15] A. Zöttl and H. Stark, *Phys. Rev. Lett.*, 2012, **108**, 218104.
[16] K. Pickl, J. Götz, K. Iglberger, J. Pande, K. Mecke, A.-S. Smith and U. Rüde, *J. of Comp. Sci.*, 2012, **3**, 374.
[17] J. W. Swan, J. F. Brady, R. S. Moore and C. 174, *Phys. Fluids*,

2011, **23**, 071901.
[18] S. Günther and K. Kruse, *EuroPhys. Lett.*, 2008, **84**, 68002.
[19] L. E. Becker, S. A. Koehler and H. A. Stone, *J. Fluid Mech.*, 2003, **490**, 15.
[20] R. Ledesma-Aguilar, H. Löwen and J. M. Yeomans, *Eur. Phys. J. E*, 2012, **35**, 70.
[21] J. E. Avron, O. Kenneth and D. H. Oaknin, *New J. Phys.*, 2005, **7**, 234.
[22] B. M. Friedrich and F. Jülicher, *Phys. Rev. Lett.*, 2012, **109**, 138102.
[23] S. Fürthauer and S. Ramaswamy, *Phys. Rev. Lett.*, 2013, **111**, 238102.
[24] M. Leoni and T. B. Liverpool, *Phys. Rev. Lett.*, 2010, **105**, 238102.
[25] E. M. Purcell, *Am. J. Phys.*, 1977, **45**, 3.
[26] R. Golestanian, T. B. Liverpool and A. Armand, *Phys. Rev. Lett.*, 2005, **94**, 220801.
[27] J. R. Howse, R. A. L. Jones, A. J. Ryan, T. Gough, R. Vafabakhsh and R. Golestanian, *Phys. Rev. Lett.*, 2007, **99**, 048102.
[28] U. M. Córdova-Figueroa and J. F. Brady, *Phys. Rev. Lett.*, 2008, **100**, 158303.
[29] R. M. Erb, N. J. Jenness, R. L. Clark and B. B. Yellen, *Adv. Mater.*, 2009, **21**, 4825.
[30] S. J. Ebbens and J. R. Howse, *Soft Matter*, 2010, **6**, 726.
[31] I. Buttinoni, G. Volpe, F. Kümmel, G. Volpe and C. Bechinger, *J. Phys.: Cond. Mat.*, 2012, **24**, 284129.
[32] P. K. Ghosh, V. R. Misko, F. Marchesoni and F. Nori, *Phys. Rev. Lett.*, 2013, **110**, 268301.
[33] M. T. Downton and H. Stark, *Eur. Phys. Lett.*, 2009, **85**, 44002.
[34] M. Arroyo, L. Heltai, D. Millán and A. DeSimone, *Proc. Natl. Acad. Sci. U.S.A.*, 2012, **109**, 17874.
[35] W. R. Schneider and R. N. Doetsch, *J. Bacteriol.*, 1974, **117**, 696.
[36] G. E. Kaiser and R. N. Doetsch, *Nature*, 1975, **255**, 656.
[37] A. Klitorinos, P. Noble, R. Siboo and E. C. S. Chan, *Oral Microbiol. Immunol.*, 1993, **8**, 242.
[38] J. D. Ruby and N. W. Charon, *FEMS Microbiol. Lett.*, 1998, **169**, 251.
[39] A. Najafi and R. Golestanian, *Phys. Rev. E*, 2004, **69**, 062901.
[40] R. Golestanian and A. Ajdari, *Phys. Rev. E*, 2008, **77**, 036308.
[41] M. Doi and S. F. Edwards, *The Theory of Polymer Dynamics*, Oxford University Press, U.S.A., 1988.
[42] F. Perrin, *J. Phys. Radium*, 1934, **5**, 497.
[43] H. C. Berg, *Random Walks in Biology*, Princeton University Press, 1983.
[44] J. Happel and H. Brenner, *Low Reynolds Number Hydrodynamics*, Prentice-Hall Inc., 1965.
[45] C. W. Oseen, *Neuere Methoden und Ergebnisse in der Hydrodynamik*, Leipzig: Akademische Verlagsgesellschaft, 1927.
[46] B. U. Felderhof, *Phys. Fluids*, 2006, **18**, 063101.